SUPPLEMENTARY INFORMATION

Photothermal Reshaping and Cavity Formation in Silica-Coated Gold Nanorods Using Nanosecond Pulsed Lasers

Tahani Albogami,[a,b] Lucien Roach,[c] Sarah Alshehri,[a,b,d] James McLaughlan,[e] Zabeada Aslam,[b,f] Zhan Ong,[a,b] Stephen D. Evans, [a,b] and Kevin Critchley* [a,b]

S1. The Porosity of Silica Coating on Gold Nanorods (AuNRs@SiO_2)

Mercadal *et al.* reported a method to determine the porosity degree of the silica shell of AuNRs@SiO_2.[1] Their method is based on the use of the extinction spectra of AuNRs@SiO_2 combined with modelling the optical properties to measure the degree of porosity of the SiO_2 shell. The principle behind determining the porosity involves placing the AuNR@SiO_2 particles in medium with increasing dielectric constant. The solvent can diffuse through silica shell pores and therefore the effective dielectric constant (ε_{eff}) of the shell is given by.

$$\varepsilon_{eff} = (1 - f)\varepsilon_{SiO_2} + f\varepsilon_m \#(Eq.\ S1)$$

where, f is the porosity fraction, ε_{SiO_2} and ε_m are the dielectric constants of silica and the medium respectively. Any change in the effective dielectric constant (ε_{eff}) of the surrounding medium causes a change in the peak position of the longitudinal surface plasmon resonance (LSPR) band to shift. It is shown that the LSPR is sensitive to the refractive index of the first few nanometres surrounding the AuNR. Thus, we applied this modelling to the optical properties of the optical properties of the AuNRs@SiO_2 used in these studies. We prepared three samples with different CTAB concentrations to prepare AuNRs@SiO_2 with a range of porosities, however, only the lowest porosity (no added CTAB) sample is presented in the main article.

CTAB was extracted using a refluxing method and the AuNRs@SiO_2 were centrifuged to form pellets, then they were dispersed into different glycerine dilutions in water in the range of 20-70% (v/v), (giving a range of ε_m from 1.768 to 2.047). They were left for 30 min stirring at room temperature to ensure good mixing and penetration of the pores. The UV-vis extinction spectra were taken for the AuNRs to define their LSPR peak positions. It was observed that the LSPR peak redshifted with increasing the glycerine concentration. This result can be explained by the change in ε_{eff} due to the loading of the pores with media of increasing ε_m with increasing glycerine content.[1] The dielectric constant of SiO_2 is represented in **Eq. S1** with ε_{SiO_2} = 2.1 and ε_m = 1.77 for water, respectively. The pores of the silica shell are assumed to be filled with a mixture whose their ε_{eff} is linearly fitted with their LSPR peak positions of AuNRs. The resonance condition of the AuNR can be approximated to:

$$-Re(\varepsilon_{Au}) = \left(\frac{1 - L_3}{L_3}\right)\varepsilon_{eff} \#(Eq.\ S2)$$

where L_3 is the depolarisation shape factor which is aspect ratio (*AR*) dependent L_3 is given by:

$$L_3 = (1 + AR)^{-1.6} \#(Eq.\ S3)$$

These approximations hold when L_3 < 0.135, and the *AR* of the both the AuNR core and AuNRs@SiO_2 are greater than 2.5 (true for all samples in this study). The LSPR peak wavelength positions were then found by looking up the wavelength at which the corresponding value occurs in the dielectric data for Au for all values of ε_m studied.[2] From the AuNR *AR* and the determined LSPR peak wavelength ε_{eff} was then determined using **Eq. S2** and **Eq. S3**. The porosity factor, f, could then be calculated using **Eq. S1**.

[a] *School of Physics & Astronomy, University of Leeds, LS2 9JT. UK.*
[b] *Bragg Centre, University of Leeds, LS2 9JT. UK.*
[c] *CNRS, ENS de Lyon, Laboratoire de Chimie (LCH, UMR 5182), 69342, Lyon, France*
[d] *Department of Physics, College of Science, University of Bisha, P.O. Box 551, Bisha 61922, Saudi Arabia.*
[e] *School of Electronic & Electrical Engineering, University of Leeds, LS2 9JT. UK*
[f] *School of Chemical & Process Engineering, University of Leeds, LS2 9JT. UK.*
* **Corresponding Author:** *Dr Kevin Critchley, k.critchley@leeds.ac.uk*

By substituting **Eq. S1** and **Eq. S3** into **Eq. S2**, **Eq. S4** can be found:

$$-Re(\varepsilon_{Au}) = \left(\frac{1-(1+AR)^{-1.6}}{(1+AR)^{-1.6}}\right)\left((1-f)\varepsilon_{SiO_2} + f\varepsilon_m\right) \#(Eq.\,S4)$$

Eq. S4 was then fitted to experimentally determined $Re(\varepsilon_{Au})$ versus ε_m values to find *f* and *AR*. This fitting was achieved using a Python script, with $Re(\varepsilon_{Au})$ converted into LSPR peak wavelength by approximating the relationship to be linear (fitted over the range used).

$$Re(\varepsilon_{Au}) = -0.0847\lambda + 43.718 \,\#\#(Eq.\,S5)$$

where, λ, is given in nm. The python code for fitting these data can be downloaded: https://github.com/kevcritc/Porosity_fit
The results are presented in **Fig S1** and the values obtained from the fits are given in **Table S1**. Our results show that for 10 mM of CTAB the porosity fraction, *f*, was 0.81. This indicates 81 % of the shell corresponds to the medium. The lower CTAB concentration of 5 mM caused a lower porosity of 0.64. Additionally, the results of AuNRs@SiO_2 that were fabricated without adding additional CTAB to the solution during the silica shell growth had a porosity of 0.43, i.e. the silica has a lower porosity. For these experiments the CTAB was extracted from the silica pores using a standard refluxing process,[3] using a mixture of ethanol and hydrochloric acid solution 50 mL and 1 mL (36 %), respectively. The sample with no additional CTAB was used in the main study and is discussed in the main report as AuNR@SiO_2

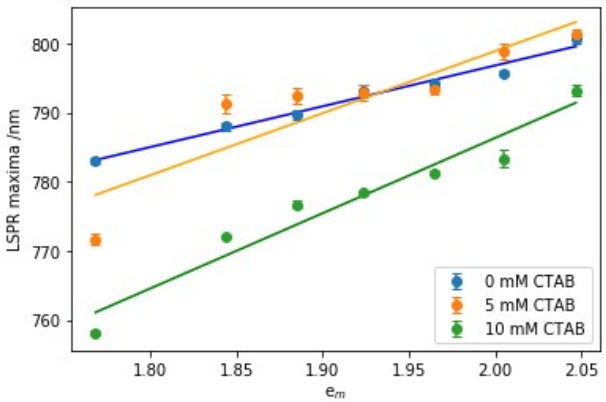

Figure S1. The relationship between the positions of LSPR peaks and ε_m the dielectric constant of the solvent mixtures of the surrounding medium. The blue line corresponds to the AuNRs@SiO_2 fabricated without adding CTAB, we assume the pores were made due to the excess CTAB in the solution. The orange line corresponds to AuNRs@SiO_2 fabricated after adding 5 mM of CTAB. The green line corresponds to AuNRs@SiO_2 produced after adding 10 mM of CTAB.

Table S1. CTAB concentrations for the AuNRs@mSiO_2, their *AR*, and *f* values correspond to the porosity degrees at each CTAB concentration. *We assume that suspensions contain some free CTAB after cleaning. The *f* values are calculated assuming that all pores are filled with surrounding mixtures.

Sample	CTAB (mM)	Slope (nm)	Error (±)	*AR*	Error (±)	*f*	Error (±)
AuNRs@SiO_2	*	59.4	3.6	3.9	0.1	0.43	0.03
AuNRs@SiO_2_5	5	90.3	19.6	3.9	0.4	0.64	0.1
AuNRs@SiO_2_10	10	110	11.7	3.8	0.2	0.81	0.1

Section S2. AuNRs@CTAB Size Analysis

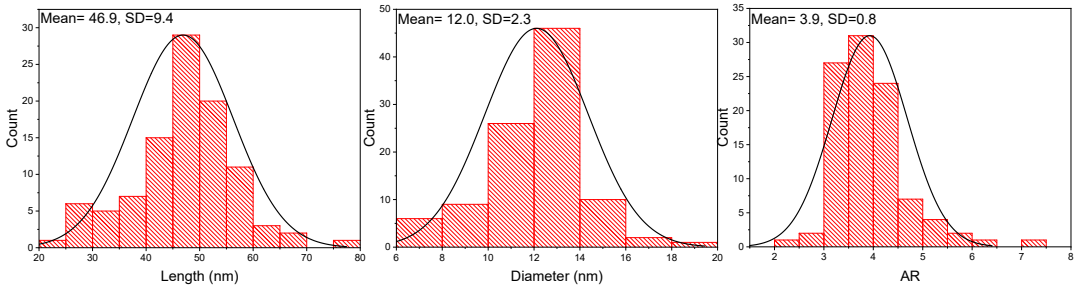

Figure S2. The size and aspect ratio (*AR*) analysis of the synthesized AuNRs

Section S3. TEM analysis of AuNRs@SiO_2 before and after exposure at 10 mJ cm^{-2}

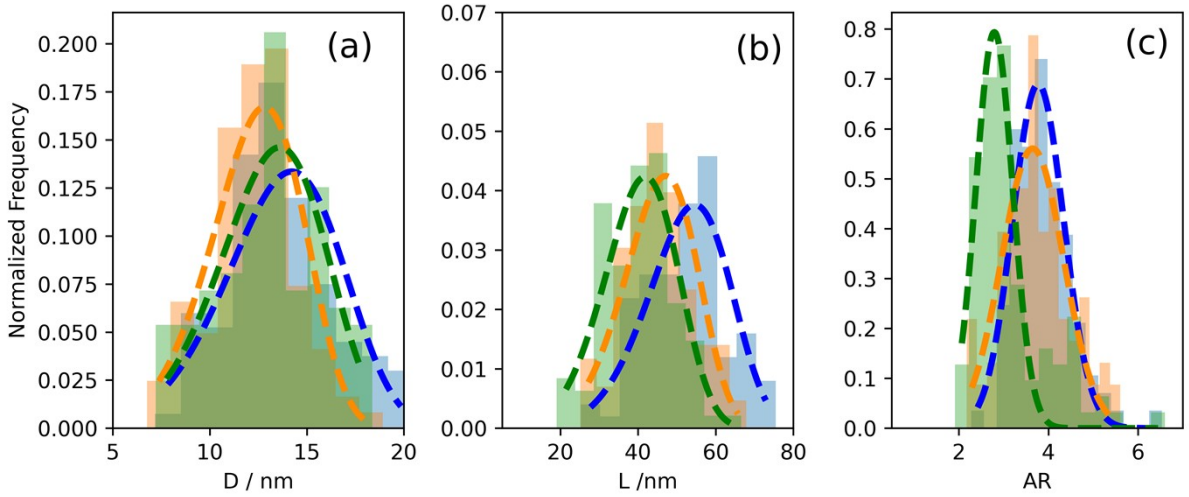

Figure S3. Histograms of the AuNR core geometry of the AuNRs@$mSiO_2$ sample before and after pulsed irradiation with a fluence of 10 mJ cm^{-2}. The histograms of the AuNR core diameters, *D* (a); lengths, *L* (b); and aspect ratios, *AR* (c) for 0 minutes (blue), 1 minute (orange), and 5 minutes (green). The dashed lines are the corresponding lines of best fit to Weibull distribution functions (n=100). The aspect ratio is as always ≥ 1.

Section S4. Changes in the Au Core Volume

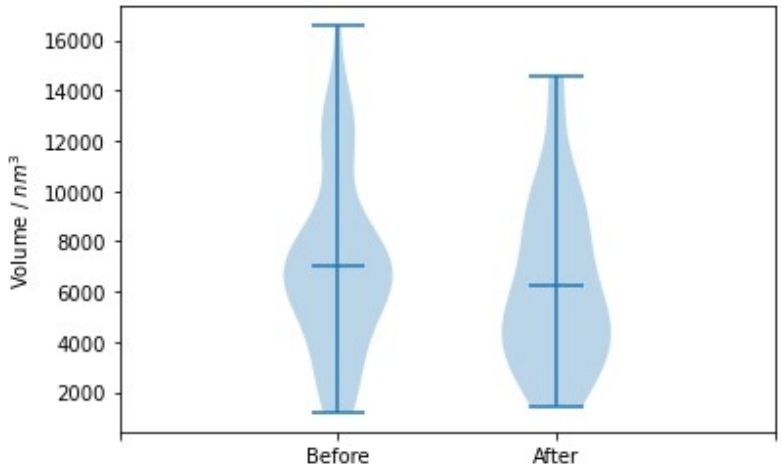

Figure S4. Violin plots of estimated volume of the Au cores from TEM images of the AuNR@SiO_2 sample before and after laser irradiation at a fluence of 20 mJ.cm^{-2}. The 2D outlines whether extracted from contours and were integrated over 180°.

Section S5. STEM and EDX Elemental Mapping of AuNRs@SiO_2

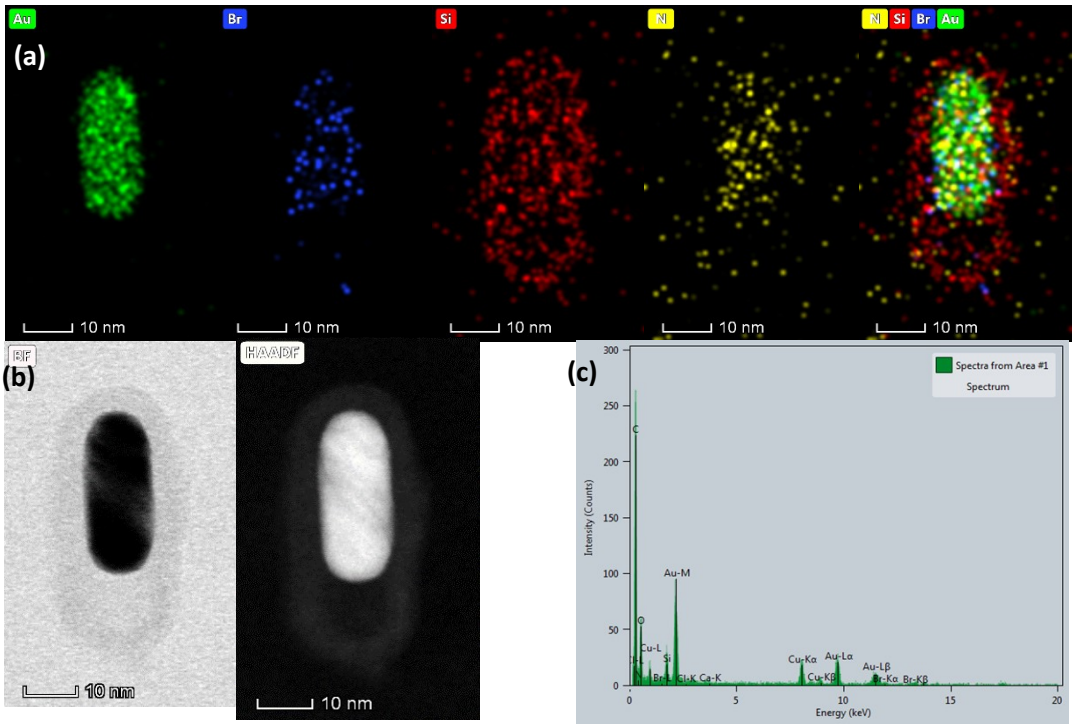

Figure S5. EDX elemental mapping of AuNR shows the core-shell elemental composition of AuNR@SiO_2 **after** laser exposure. **(a)** STEM-HAADF, Au, N, Br, Si, and their overlaid image respectively. The scale bar represents 20 nm. **(b)** EDX line scanning of AuNR@SiO_2 (**Inset:** EDX line scanning profile of cross section of AuNR@SiO_2). The inset image indicates the area of AuNR@SiO_2 that were used to measure the signal intensity of Au, Si, N, and Br. **(c)** Corresponding EDX spectra of AuNR@SiO_2 supported on a copper grid. SiO_2 shell thickness about 7.0 ± 0.2 nm. (**Scale bar:** 20 nm).

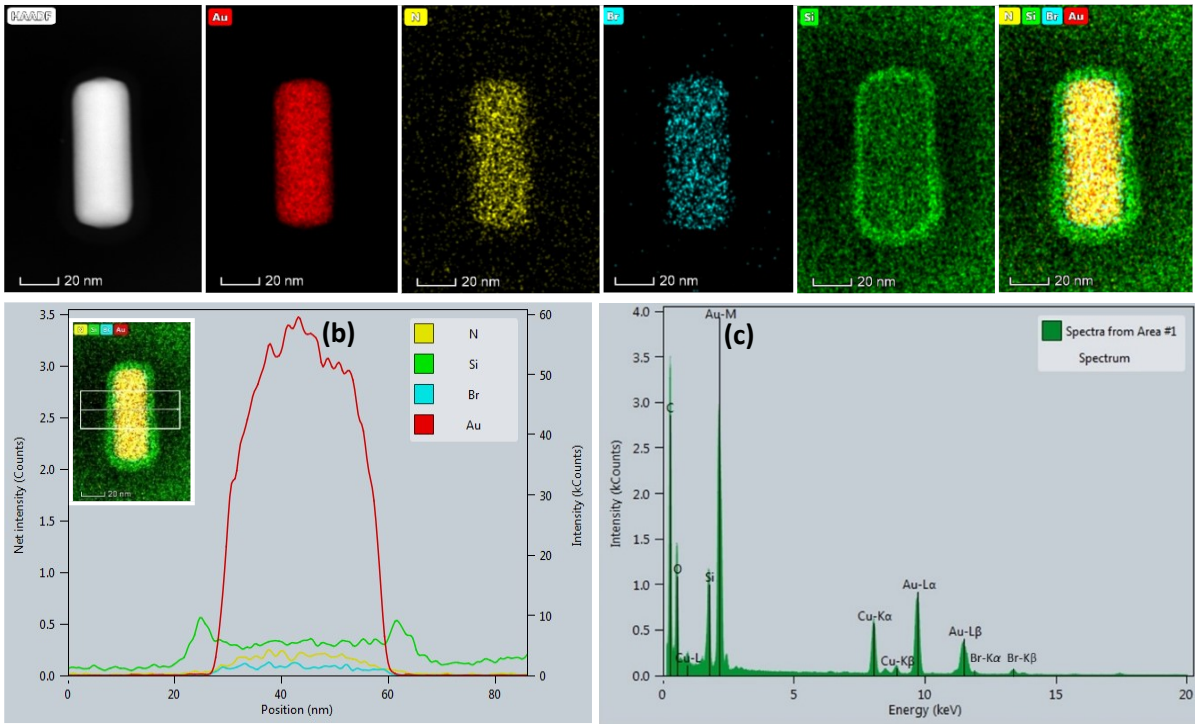

Figure S6. EDX elemental mapping of AuNR **before** laser exposure shows the core-shell elemental composition of AuNR@SiO_2. **(a)** STEM-HAADF, Au, N, Br, Si, and their overlaid image respectively. The scale bar represents 20 nm. **(b)** EDX line scanning of AuNR@SiO_2 (**Inset:** EDX line scanning profile of cross section of AuNR@SiO_2). The inset image indicates the area of AuNR@SiO_2 that were used to measure the signal intensity of Au, Si, N, and Br. **(c)** Corresponding EDX spectra of AuNR@SiO_2 supported on a copper grid. (**Scale bar:** 20 nm).

Section S6. Off-Resonance Change in End Cap Factor

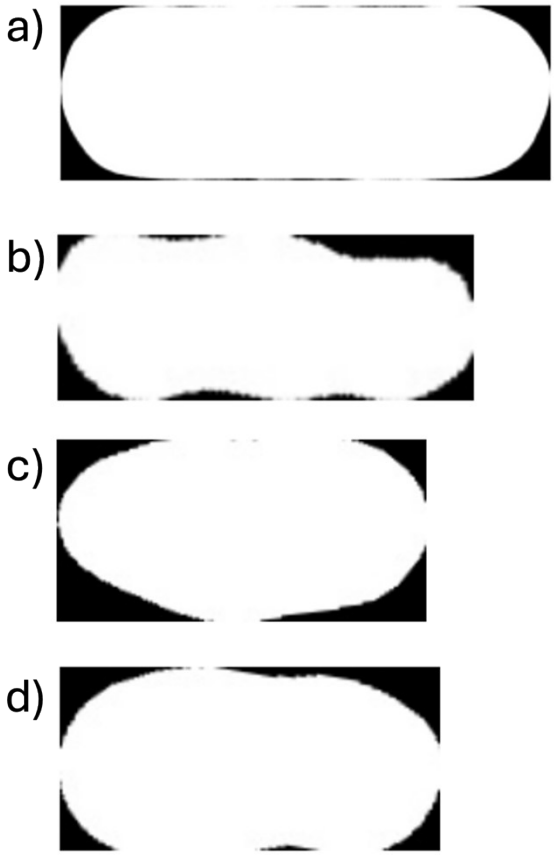

Figure S7. Representative images from clustering results of hierarchical clustering of TEM Images of the Au core of AuNRs@SiO_2 post ns-pulsed laser exposure (no scale). The contour images were rotated and aligned before being embedded 16-layer recognition model. The representative images can be called a) nanorod, b) irregular rod, c) ovaloid, and d) dumbbell.

Section S7. Modelling of the electromagnetic and thermal response of the AuNRs

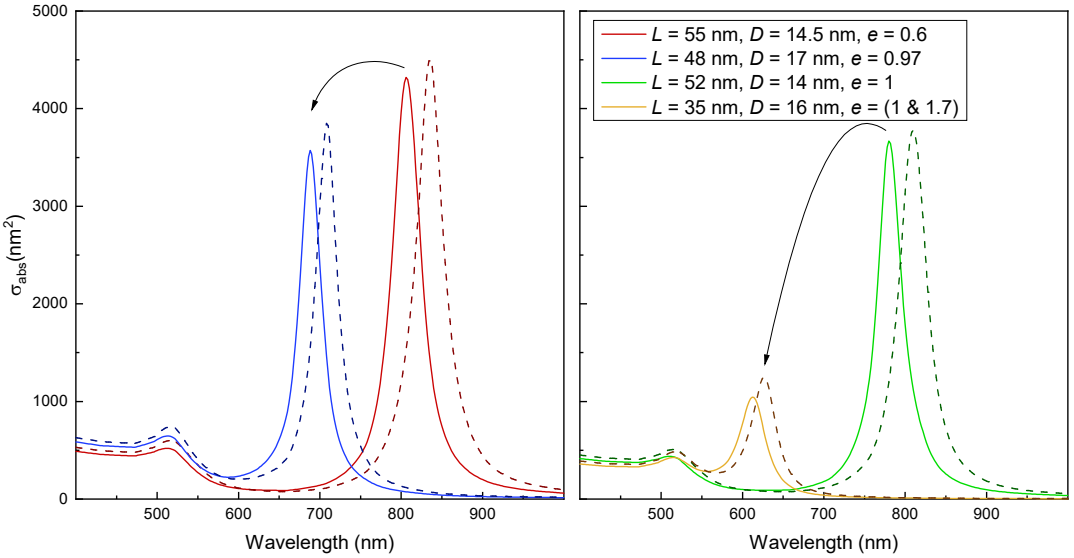

Figure S8. Simulated spectra with associated geometries below

Simulated geometries.

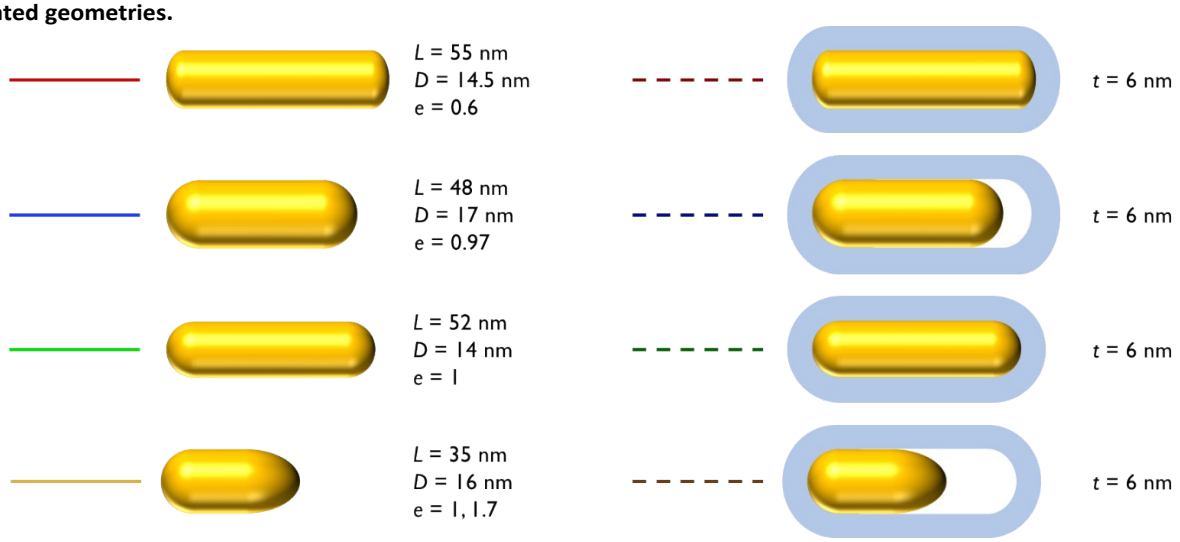

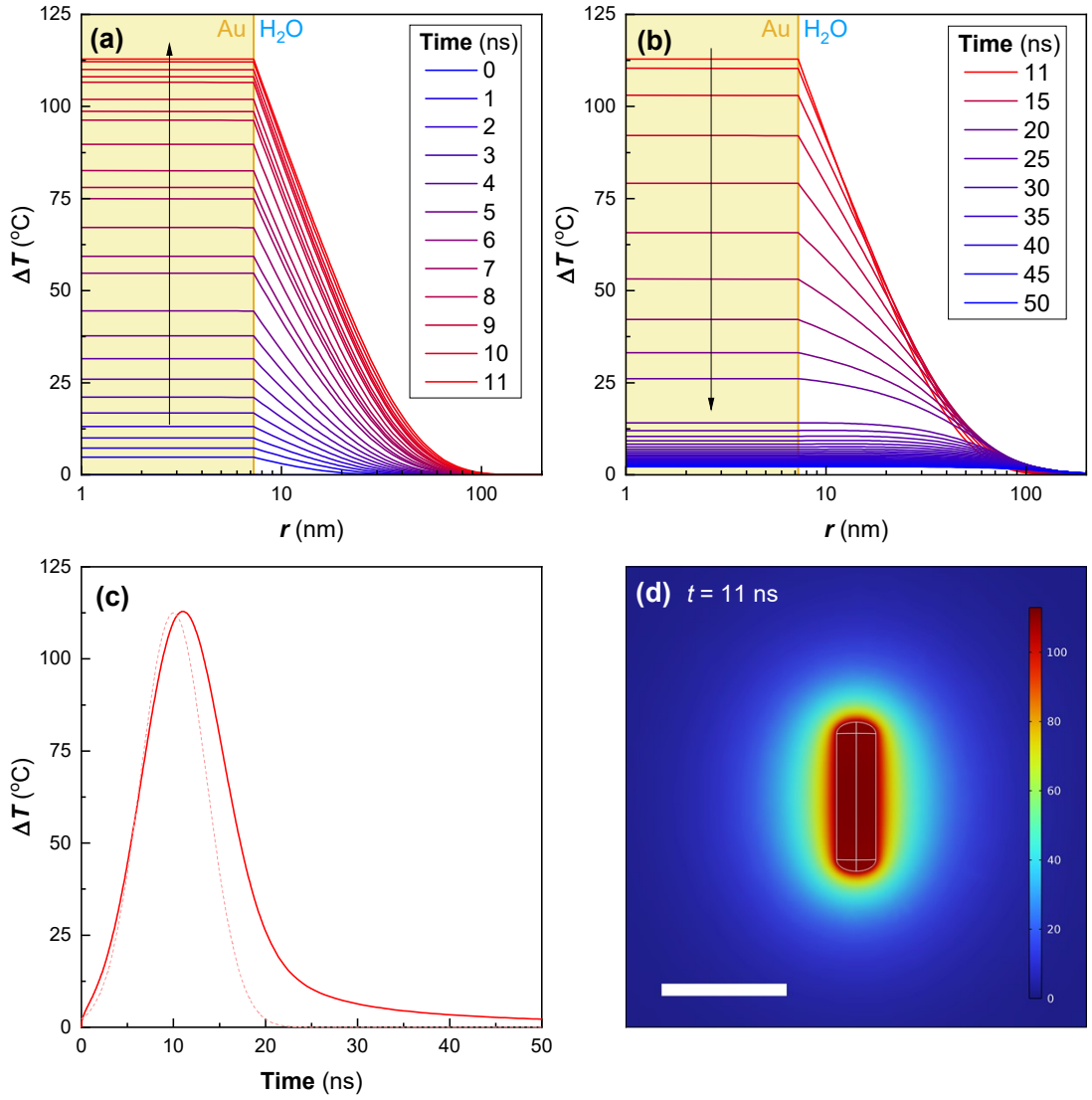

Figure S9. Simulated temperature profiles for a AuNR (D = 14.5 nm, L = 55 nm, $e_1 = e_2$ = 0.6) **without** a silica shell illuminated by a 5 mJ cm^{-2} laser pulse. Heating profiles during which the temperature of the AuNR is (a) increasing and (b) decreasing. Temperature was measured along an axis orientated longitudinally from the centre of the AuNR. (c) Temperature at r = 0 (inside the AuNR) over 50 ns. The dashed line is the profile of the laser pulse. (d) Temperature map at t = 11 ns (peak AuNR temperature). The geometry of the AuNR is represented in white. Colour scale is ΔT in °C. The scale bar represents 50 nm.

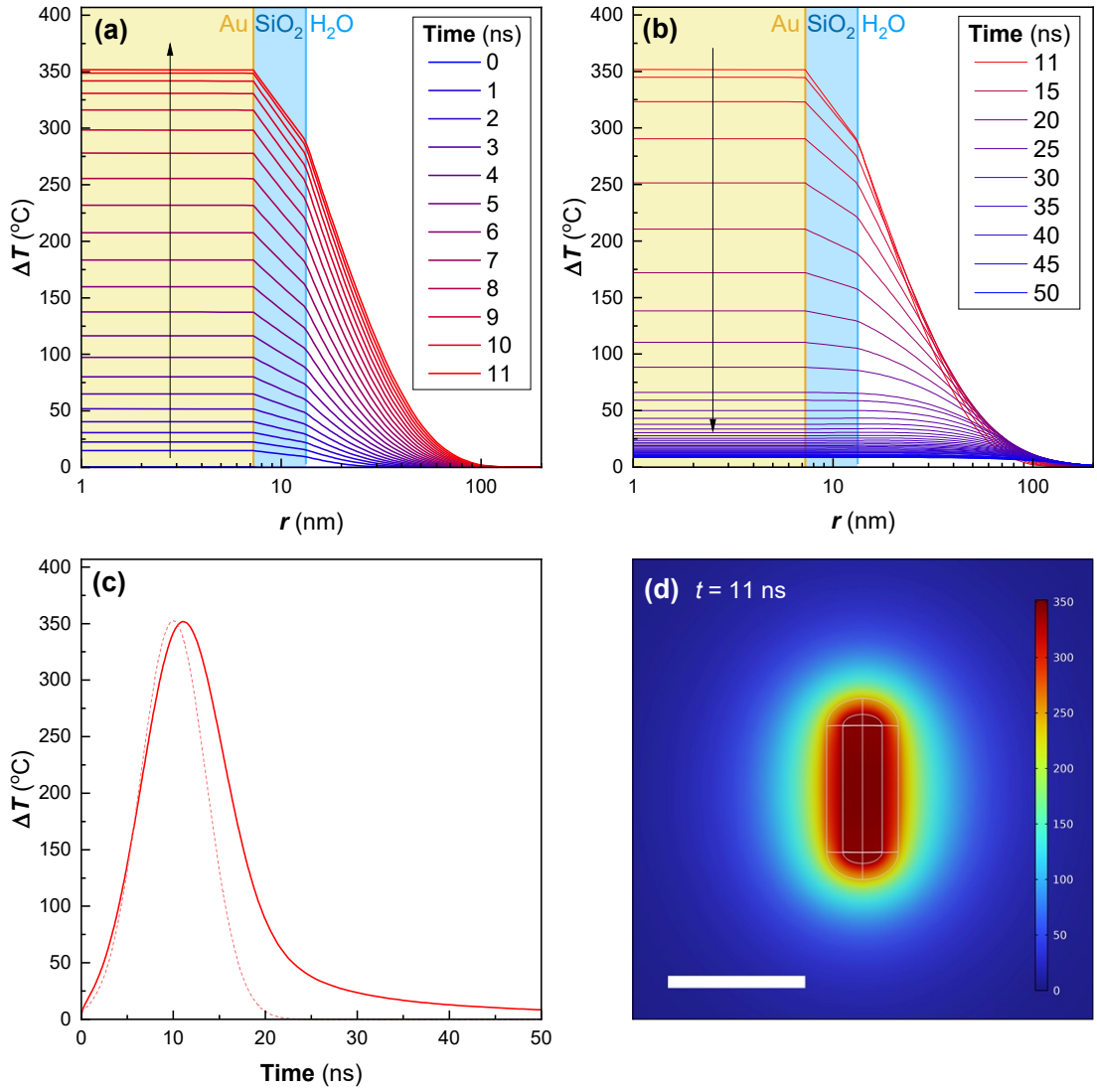

Figure S10. Simulated temperature profiles for a AuNR (D = 14.5 nm, L = 55 nm, $e_1 = e_2$ = 0.6, *i.e.* the same as Fig. S9 **with** a silica shell of 6 nm in thickness. Heating profiles which the temperature of the AuNR is (a) increasing and (b) decreasing. Temperature was measured along an axis orientated longitudinally from the centre of the AuNR. (c) Temperature at r = 0 (inside the AuNR) over 50 ns. The dashed line is the profile of the laser pulse. (d) Temperature map at t = 11 ns (peak AuNR temperature). The geometry of the AuNR@SiO_2 is represented in white. Colour scale is ΔT in °C. The scale bar represents 50 nm.

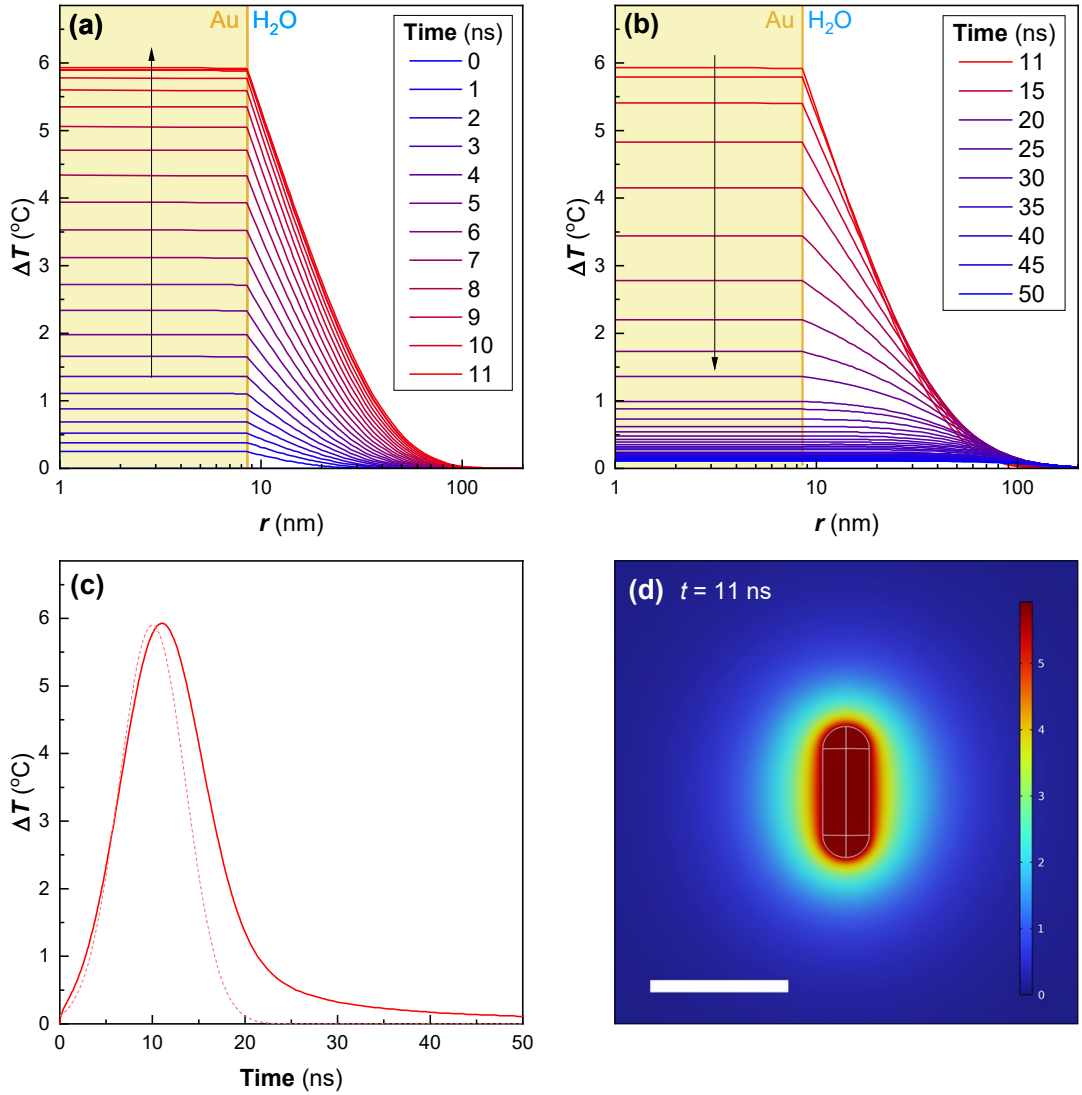

Figure S11. Simulated temperature profiles for a AuNR (D = 17 nm, L = 48 nm, e_1 = 0.6, e_2 = 0.92) without a silica shell. This is the reshaped morphology of the AuNR simulated in Figs. S9 & S10. Heating profiles which the temperature of the AuNR is (a) increasing and (b) decreasing. Temperature was measured along an axis orientated longitudinally from the centre of the AuNR. (c) Temperature at r = 0 (inside the AuNR) over 50 ns. The dashed line is the profile of the laser pulse. (d) Temperature map at t = 11 ns (peak AuNR temperature). The geometry of the AuNR is represented in white. Colour scale is ΔT in °C. The scale bar represents 50 nm..

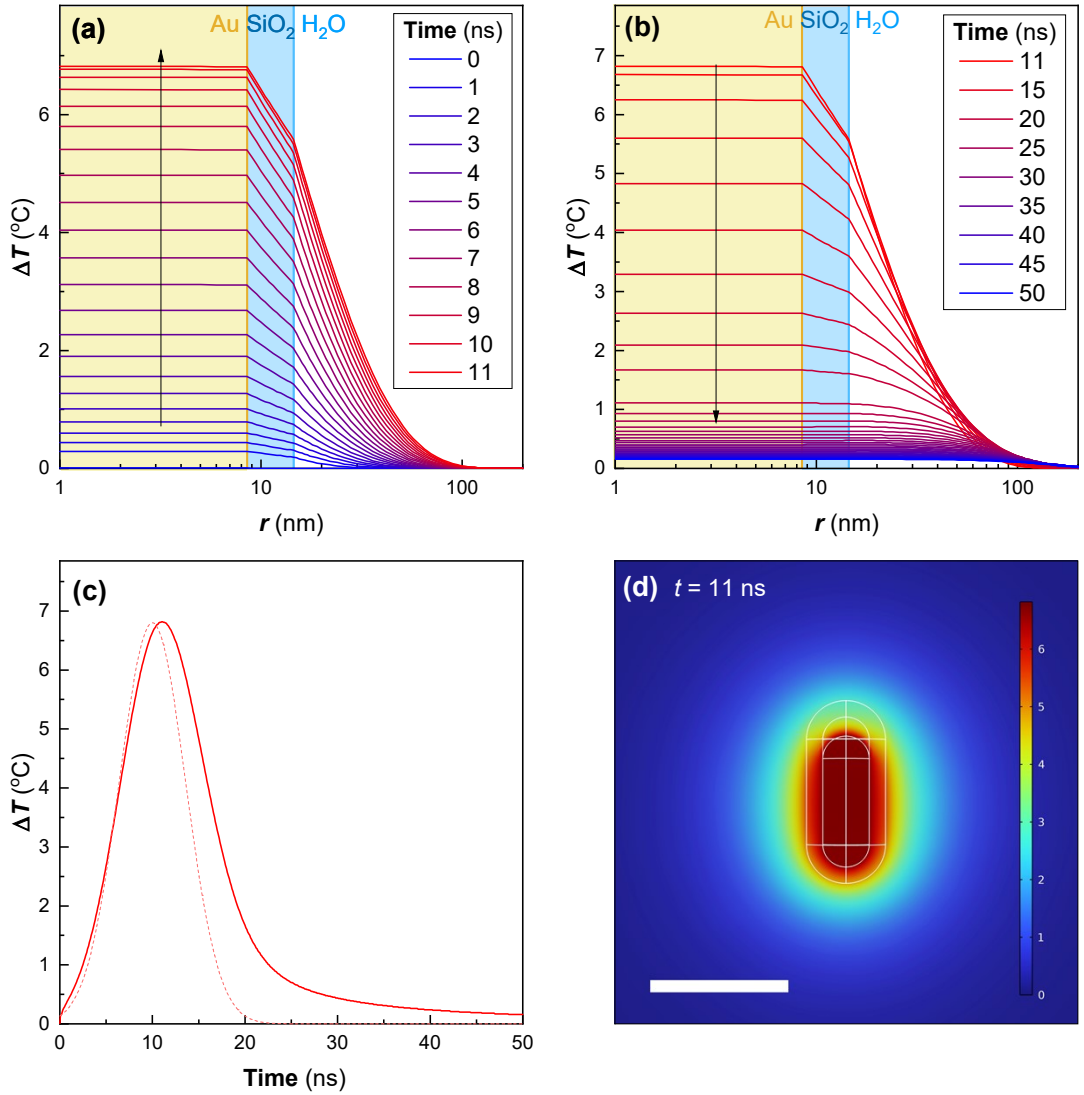

Figure S12. Simulated temperature profiles for a AuNR (D = 17 nm, L = 48 nm, e_1 = 0.6, e_2 = 0.92, *i.e.* the same as Fig. S11) **with** a silica shell of 6 nm in thickness containing an internal cavity 55 nm in length (*i.e.* 7 nm of the length are not occupied by the reshaped AuNR). This is the reshaped morphology of the AuNR simulated in Figs. S9 & S10. Heating profiles which the temperature of the AuNR is (a) increasing and (b) decreasing. Temperature was measured along an axis orientated longitudinally from the centre of the AuNR. (c) Temperature at r = 0 (inside the AuNR) over 50 ns. The dashed line is the profile of the laser pulse. (d) Temperature map at t = 11 ns (peak AuNR temperature). The geometry of the AuNR@SiO_2 is represented in white. Colour scale is ΔT in °C. The scale bar represents 50 nm.

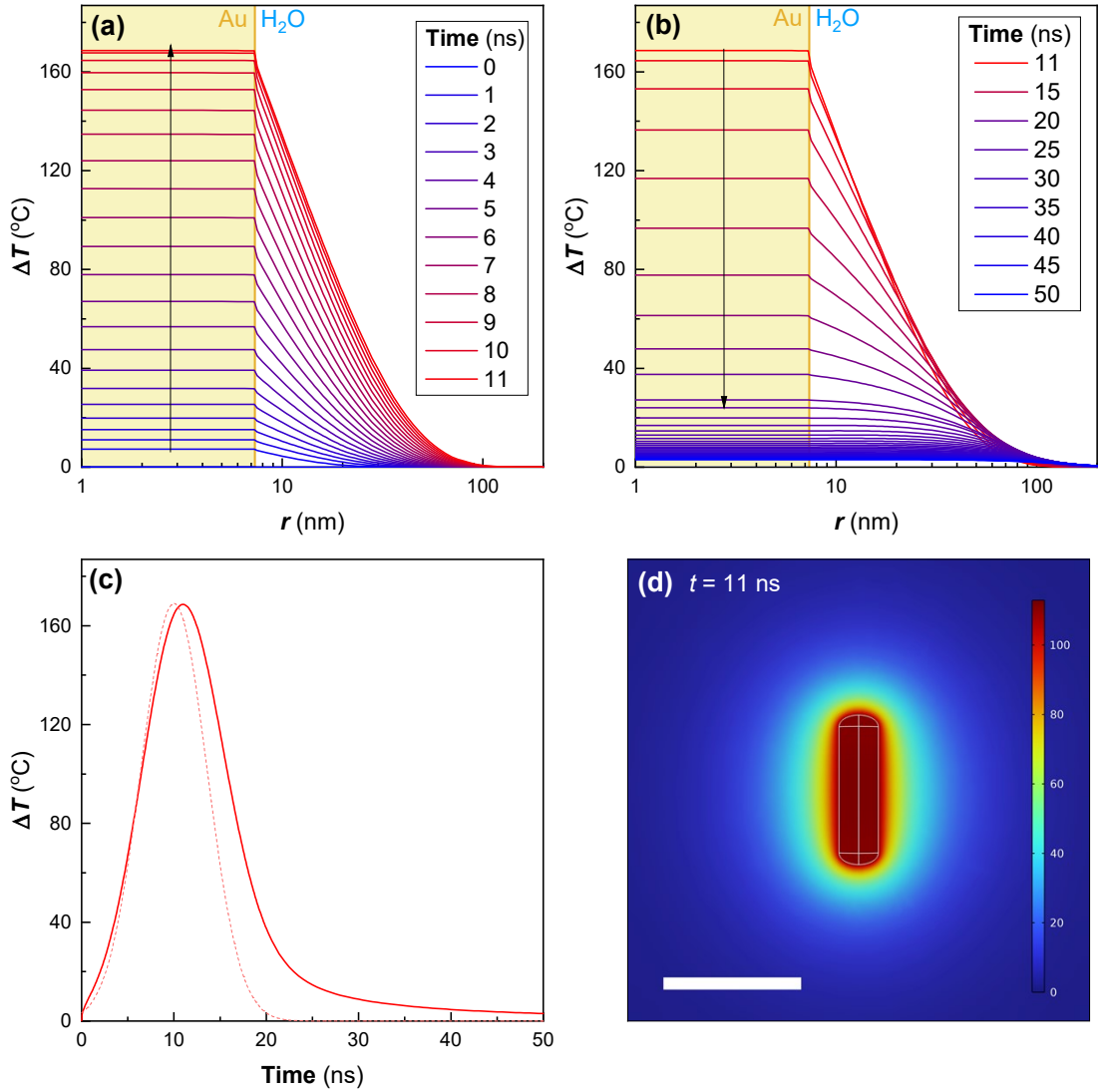

Figure S13. Simulated temperature profiles for a AuNR (D = 14 nm, L = 52 nm, $e_1 = e_2 = 1$) **without** a silica shell illuminated by a 20 mJ cm^{-2} laser pulse. Heating profiles which the temperature of the AuNR is (a) increasing and (b) decreasing. (c) Temperature at r = 0 (inside the AuNR) over 50 ns. The dashed line is the intensity profile of the laser pulse. Temperature was measured along an axis orientated longitudinally from the centre of the AuNR. (d) Temperature map at t = 11 ns (peak AuNR temperature). The geometry of the AuNR is represented in white. Colour scale is ΔT in °C. The scale bar represents 50 nm. (d) Temperature map at t = 11 ns (peak AuNR temperature). The geometry of the AuNR is represented in white. Colour scale is ΔT in °C. The scale bar represents 50 nm.

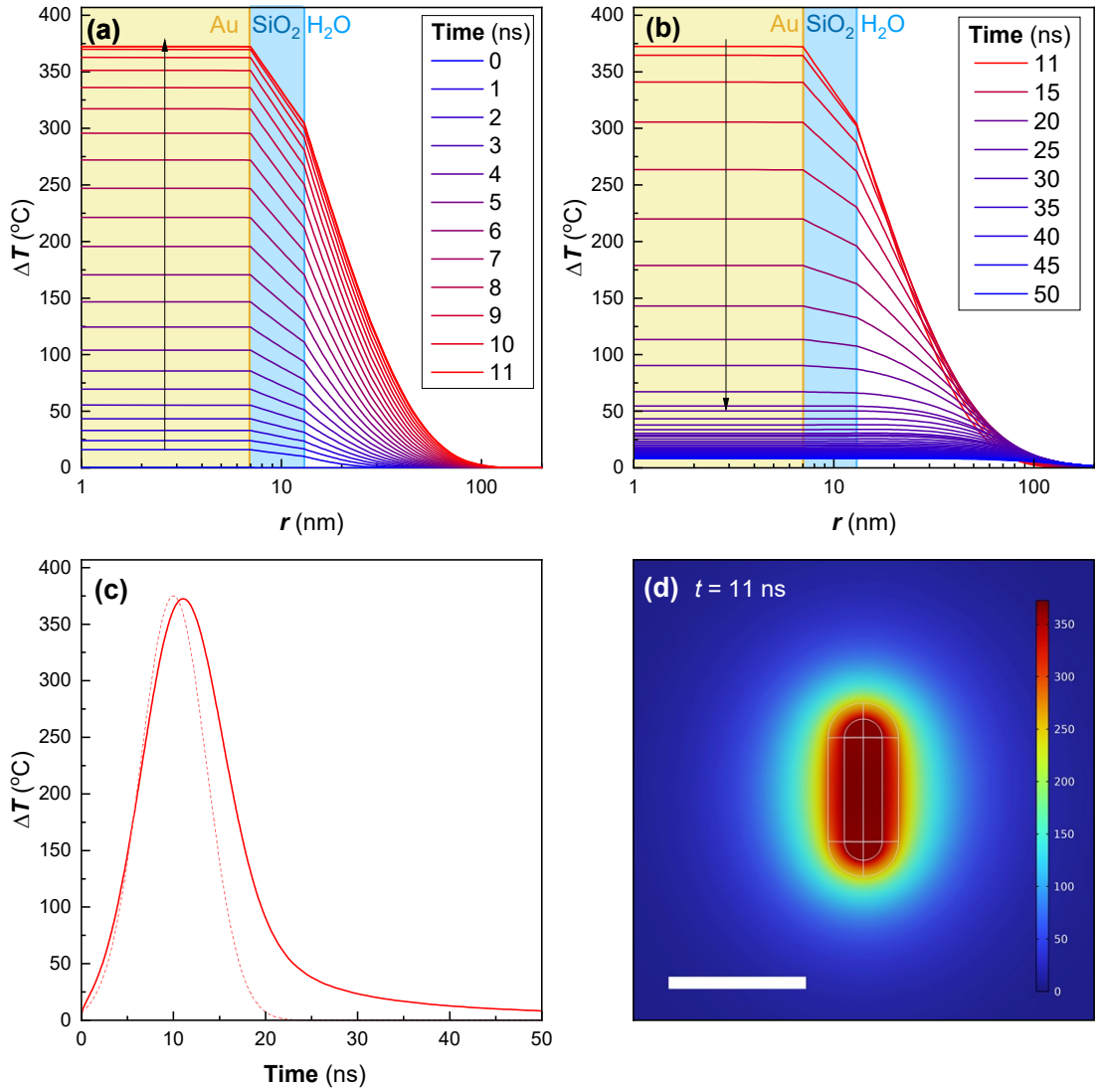

Figure S14. Simulated temperature profiles for a AuNR (D = 14 nm, L = 52 nm, e_1 = e_2 = 1, *i.e.* the same as Fig. S13) **with** a silica shell of 6 nm in thickness illuminated by a 20 mJ cm^{-2} laser pulse. Heating profiles which the temperature of the AuNR is (a) increasing and (b) decreasing. (c) Temperature at r = 0 (inside the AuNR) over 50 ns. The dashed line is the intensity profile of the laser pulse. (d) Temperature map at t = 11 ns (peak AuNR temperature). The geometry of the AuNR is represented in white. Colour scale is ΔT in °C. The scale bar represents 50 nm. (d) Temperature map at t = 11 ns (peak AuNR temperature). The geometry of the AuNR@SiO_2 is represented in white. Colour scale is ΔT in °C. The scale bar represents 50 nm.

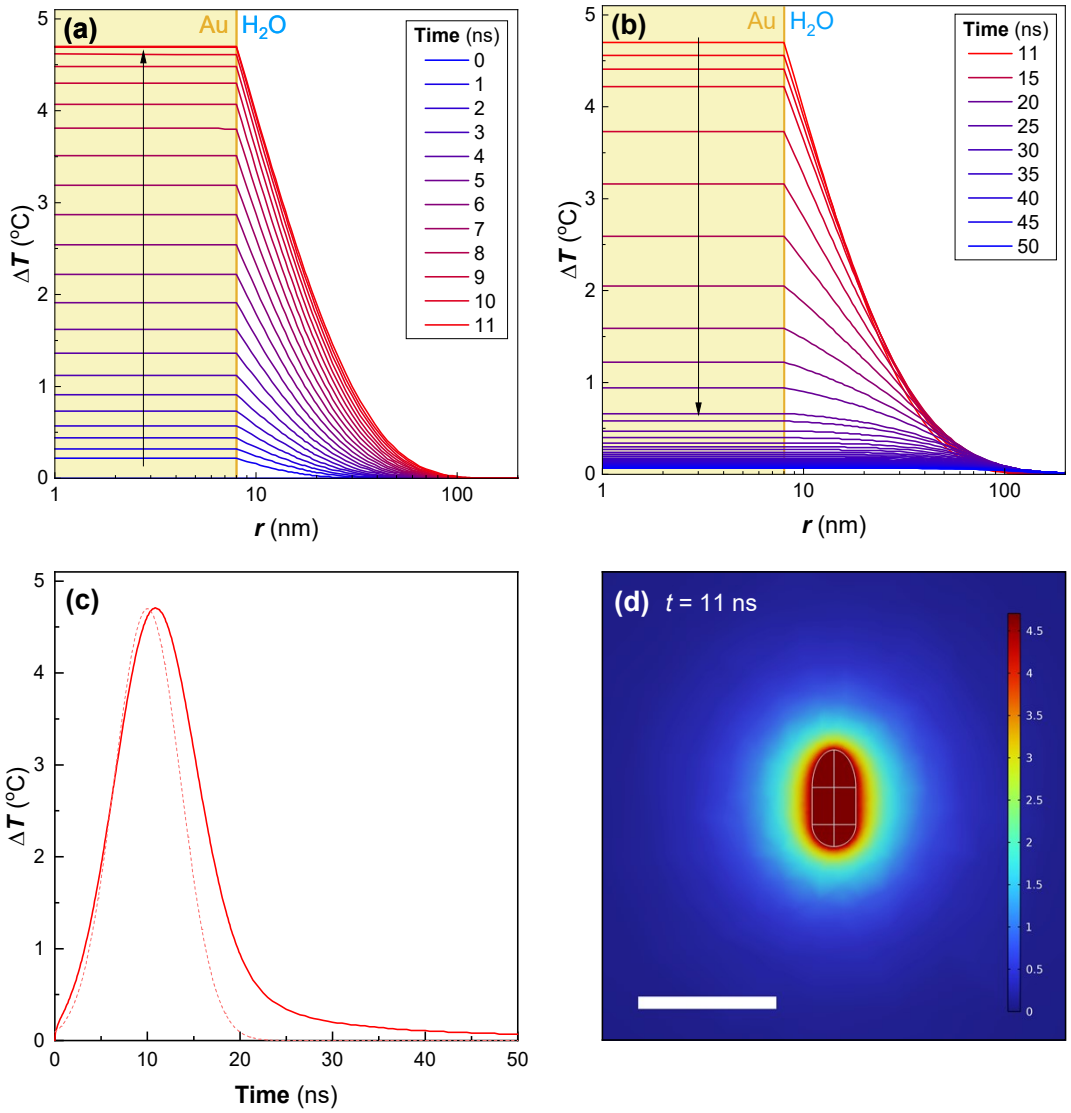

Figure S15. Simulated temperature profiles for a AuNR (D = 16 nm, L = 35 nm, e_1 = 1.0, e_2 = 1.7) **without** a silica shell in thickness illuminated by a 20 mJ cm^{-2} laser pulse. This is the reshaped morphology of the AuNR simulated in Figs. S13 & S14. Heating profiles which the temperature of the AuNR is (a) increasing and (b) decreasing. (c) Temperature at r = 0 (inside the AuNR) over 50 ns. The dashed line is the profile of the laser pulse. (d) Temperature map at t = 11 ns (peak AuNR temperature). The geometry of the AuNR is represented in white. Colour scale is ΔT in °C. The scale bar represents 50 nm. (d) Temperature map at t = 11 ns (peak AuNR temperature). The geometry of the AuNR is represented in white. Colour scale is ΔT in °C. The scale bar represents 50 nm.

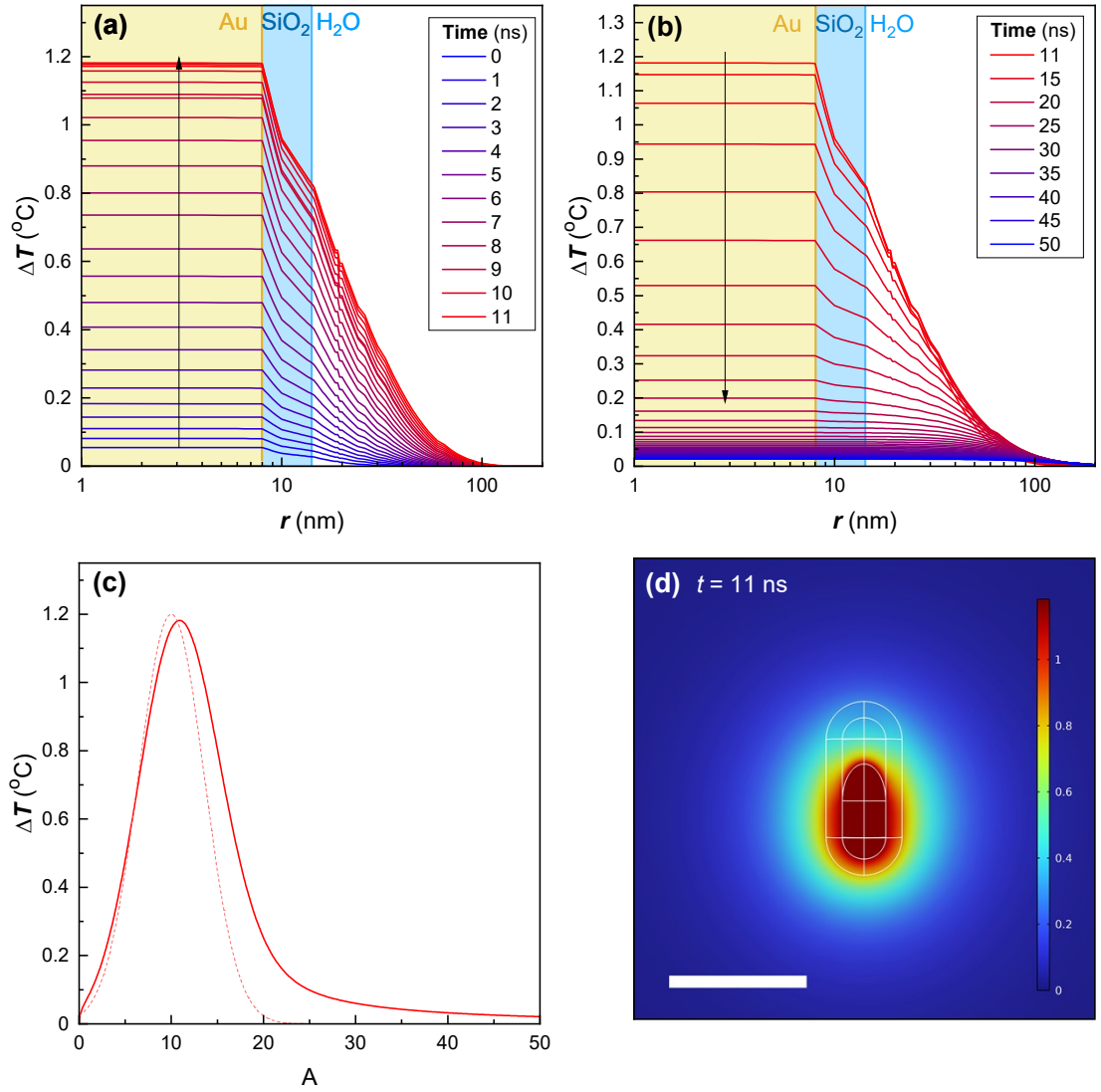

Figure S16. Simulated temperature profiles for a (D = 16 nm, L = 35 nm, e_1 = 1.0, e_2 = 1.7, *i.e.* the same as Fig. S15) **with** a silica shell of 6 nm in thickness containing an internal cavity 52 nm in length (*i.e.* 17 nm of the length are not occupied by the reshaped AuNR) illuminated by a 20 mJ cm^{-2} laser pulse. This is the reshaped morphology of the AuNR simulated in Figs. S13 & S14. Heating profiles which the temperature of the AuNR is (a) increasing and (b) decreasing. (c) Temperature at r = 0 (inside the AuNR) over 50 ns. The dashed line is the profile of the laser pulse. (d) Temperature map at t = 11 ns (peak AuNR temperature). The geometry of the AuNR@SiO_2 is represented in white. Colour scale is ΔT in °C. The scale bar represents 50 nm

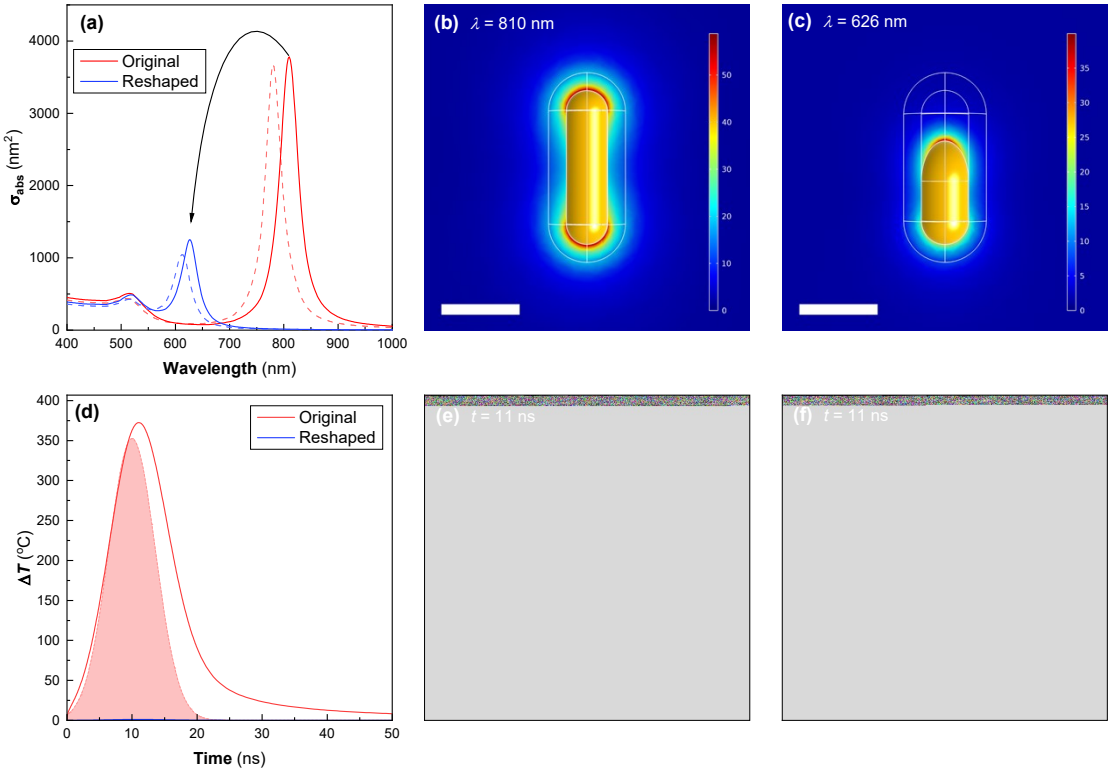

Figure S17 (a) FEM simulated absorbance spectra of AuNRs@SiO_2 particles. The dashed lines are the spectra of the AuNR cores without a SiO_2 coating. Electric field enhancement maps for **(b)** original AuNR@SiO_2 at λ = 836 nm and **(c)** reshaped AuNR@SiO_2 at λ = 705 nm. The scale bar for (b) and (c) is 25 nm. **(d)** Temperature of the AuNR core of both AuNR@SiO_2 particles illuminated by a 5 mJ cm^{-2}, 850 nm, 7 ns laser pulse centered on t = 10 ns as a function of time. The profile of the laser pulse is shown as the shaded area. **(e)** Temperature map of the original AuNR@SiO_2 at t = 11 ns (1 ns after the peak of the laser pulse). (f) Temperature map of the reshaped AuNR@SiO_2 at t = 11 ns. The scale bar for (e) and (f) is 25 nm.

Section S8. Post-Irradiation End Cap Factor

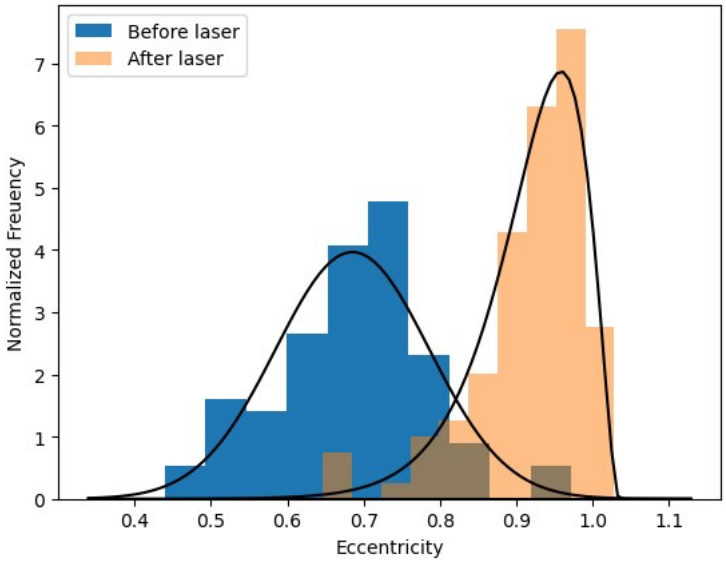

Figure S18. A histogram of the end cap factor of the gold nanorod tips before and after ns pulsed laser exposure at 5 mJ cm^{-2} (λ = 850 nm). The histograms are fitted to a beta functional although it should be noted that the before distribution fits just as well to a normal distribution. The FWHM of before and after are 0.34 and 0.35, respectively.

References

1 PA Mercadal, LA Perez and EA Coronado, *J. Phys. Chem. C*, **2021**, *125*, 15516.
2 PB Johnson and RW Christy, *Phys. Rev. B*, **1972**, *6*, 4370.
3 T Kobayashi, D Singappuli-Arachchige, Z Wang, II Slowing and M Pruski, *Phys. Chem. Chem. Phys.*, **2017**, *19*, 1781.